Phase-amplitude markers of synchrony and noise: A resting-state and TMS-EEG study of schizophrenia

D Freche[1,2], J Naim-Feil[3,2], S Hess[4,5], A Peled[6,7], A Grinshpoon[6,7], E Moses[2], and N Levit-Binnun[1,*]

[1] *Sagol Center of Brain and Mind, Ivcher School of Psychology, Interdisciplinary Center (IDC) Herzliya, Israel*
[2] *Department of Physics of Complex Systems, Weizmann Institute of Science, Israel*
[3] *Turner Institute for Brain and Mental Health, School of Psychological Sciences and Monash Biomedical Imaging, Monash University, Clayton, Australia*
[4] *Geha Mental Health Center, Petah Tikvah, Israel*
[5] *Sackler Faculty of Medicine, Tel Aviv University, Ramat Aviv, Israel*
[6] *Rappaport Faculty of Medicine, Technion*
[7] *Institute for Psychiatric Studies, Shaar Menashe Mental Health Center, Israel*
[*] *Corresponding author: navalb@idc.ac.il*

Abstract

The electroencephalogram (EEG) of schizophrenia patients exhibits several well-known abnormalities. For brain responses evoked by a stimulus in a variety of behavioral paradigms, these alterations appear as a reduction of signal-to-noise ratio and of phase-locking, and as a facilitated excitability. Here we observe these effects in EEG using transcranial magnetic stimulation (TMS)-evoked potentials, comparing also to the resting-state EEG. To ensure veracity of our results we used three weekly sessions and analyzed both resting state and TMS-EEG data. In addition to confirming the known results for the stimulus response we also show a broadening of the amplitude distribution in the resting-state EEG of patients relative to that of controls, indicative of lower signal to noise. Specifically, we evaluated the instantaneous amplitude in narrow-band filtered EEG, using a form of mean-normalized variation (quartile coefficient, QC) as a marker for amplitude fluctuations. We find that on time scales of seconds to tens of seconds, amplitude fluctuations in the alpha and beta frequency bands in the resting state of healthy controls are larger than their fluctuations in schizophrenia patients. According to our marker, the narrow-band-filtered amplitude fluctuations in the patient group are more similar to the theoretical limit of narrow-band Gaussian noise. Our results thus support the neuronal noise hypothesis of schizophrenia, which states that the ability of neuronal populations to form locally and temporally correlated activity is reduced in schizophrenia due to inherent noise in all brain activity.

1 Introduction

Schizophrenia is a mental disease with a complex pathology that dynamically evolves across the adult lifespan (Krystal et al., 2017). Several decades of research in schizophrenia have provided extensive evidence to the pervasive, globally occurring structural, physiological, functional and genetic abnormalities that characterizes the disorder. Abnormalities of brain tissue structure from the scale of synapses to whole brain regions have been described, with connectivity degradation occurring both locally and long-range. Correspondingly, a range of profound functional abnormalities were observed in activity, from cell assemblies to large-scale networks (Uhlhaas and Singer, 2010; Krystal et al., 2017).

One way to probe the functional abnormalities in schizophrenia is by studying dynamics of brain activity using EEG in stimulus-response paradigms. Generally, the main alterations of evoked responses in schizophrenia concern reductions in amplitudes and in phase locking (Winterer et al., 2000a, 2004; Spencer

et al., 2003; Frantseva et al., 2012; Shin et al., 2015), as well as facilitated excitation in late-stage response (Radhu et al., 2015; Frantseva et al., 2012; Rogasch et al., 2014), increased inter-trial variability (Winterer et al., 2000a, 2004), and altered spectral power (Winterer et al., 2000a; Frantseva et al., 2012).

A hypothesis to explain these findings heuristically, first formulated by Winterer et al. (2000a), suggests the presence of inherent noise in brain activity. This manifests itself as stimulus-unrelated background activity that interferes with stimulus-evoked responses and thus leads to increased inter-trial variability. Further work by Rolls et al. (2008) conceptualized this hypothesis within a dynamical systems framework, with altered stability properties of attractors. Krystal et al. (2017) suggested that although the large inter-trial variability observed in schizophrenia can result from random background activity that degrades regular signals, it may also lead in itself to the creation of an aberrant signal. This suggests that not only evoked activity should be affected by such noise, but that the resting state activity in schizophrenia should exhibit correlates of abnormal activity as well. Indeed, various alterations of the resting-state EEG in schizophrenia have been reported. General findings include alterations of power spectra (Uhlhaas and Singer, 2010) and abnormalities of spatial activity in analyses of microstates (Rieger et al., 2016; Michel and Koenig, 2018). Notably, temporal activity alterations in long-range time correlations (LRTC) (Nikulin et al., 2012) were found, demonstrating that brain activity in patients shows reduced temporal auto-correlations on the timescale of tens of seconds.

This hypothesis, that noise and its regulation is at the heart of alterations of functional activity in schizophrenia, has been suggested as a low-level mechanism to explain both physiological and behavioral findings (Northoff and Duncan, 2016; Winterer et al., 2000a; Rolls et al., 2008). Alterations in global activity can shape the processing of stimulus-induced activity and may provide the basis for the reported changes in cognitive, affective and social functions (Northoff and Duncan, 2016). Ultimately, these alterations may underlie the unstable symptoms and symptom severity characteristic of the disorder (Habtewold et al., 2019; Bota et al., 2011). Despite the apparent popularity of the noise hypothesis, the fundamental question regarding the nature of this postulated noise remains to be answered. This regards its origins at the molecular, synaptic, or cellular level, as well as its properties, such as more deterministic or more random characteristics, leading to different interpretations of variability in brain activity (Faisal et al., 2008).

In this paper, we provide evidence supporting the noise hypothesis, which we formulate such that it applies to brain activity in response to a stimulus as well as in resting state: The presence of noise is a characteristic of brain activity in schizophrenia, which reduces the capacity of the brain to achieve the formation of spatially and temporally stable correlated activity in neuronal populations. We therefore consider phase and amplitude markers derived from the EEG which can be viewed as measures for correlations in population activity. We record TMS-evoked and resting-state EEG activity in schizophrenia patients and healthy controls, with three repetitions for each participant. Evaluating both groups three times with one week between each session strengthens the reliability of our results (see also (Kerwin et al., 2018)), as cortical responses may vary with changes in symptoms (Naim-Feil et al., 2019). The advantage of inducing cortical activation with TMS and measuring responses with EEG is that it does not require active participation and attention of the schizophrenia patients (Daskalakis et al., 2002; Rogasch et al., 2014).

In the TMS-EEG experiments presented here we find a reduced signal-to-noise ratio, reduced phase locking to the TMS-pulse, and facilitated post-response excitability in schizophrenia as compared to healthy controls. This confirms previous reported findings with our data. In the resting-state EEG experiments, we look at EEG signal amplitudes. We provide an analysis of amplitude averages and amplitude fluctuations on the timescale of tens of seconds. Generally, we find that these fluctuations are less variable in patients and, in terms of our marker, are closer to noise fluctuations. We suggest to interpret this finding as a reduced ability to create stable spatiotemporal correlations of brain activity. Finally, our overall findings are reviewed in the context of the current discussion about possible constituents of brain activity alterations in schizophrenia.

2 Materials and methods

The study was approved by the Shaar Menashe Mental Health Center Institutional Review Board. All participants were reimbursed the equivalence of 35 US dollars for participating in each EEG recording sessions.

2.1 Subjects

Thirty healthy controls without any history of psychiatric illness, drug abuse or head injury were recruited through local advertisements. Three subjects were excluded because not all three sessions were attended, yielding 27 datasets for control.

Thirty in-unit schizophrenia patients at Shaar Menashe Mental Health Center qualified for the study according to DSM IV-TR Schizophrenia (DSM, 2000). Nine subjects were excluded because not all three sessions were attended, yielding 21 datasets of schizophrenia patients. Each patient was evaluated by a trained psychiatrist using the Scale for the Assessment of Positive Symptoms (SAPS) and the Scale for the Assessment of Negative Symptoms (SANS) to quantify clinical symptoms of schizophrenia (Andreasen, 1984, 1989).

All subjects completed a general demographic questionnaire and TMS safety questionnaire (Rossi et al., 2011). For demographic and clinical data, see Table 1. Each recording session was supervised by a trained psychiatrist, who assured that epileptic activity was absent in the EEG of all subjects.

	Patients	Controls
Number of subjects	21	27
Gender (m + f)	19 + 2	21 + 6
Age (years)	40 ± 8	35 ± 11

Duration of illness (years)	21 ± 8		
Antipsychotics	typical	atypical	combination
No. (percentage) of patients	7 (33 %)	12 (57 %)	2 (10 %)
	28±16		
	89±20		

	Session 1	Session 2	Session 3
SAPS global	11.0 ± 5.2	10.0 ± 4.2	9.8 ± 5.3
(a) Hallucinations	3.0 ± 2.4	2.9 ± 2.1	2.6 ± 2.1
(b) Delusions	6.3 ± 7.7	5.3 ± 6.1	4.9 ± 5.7
(c) Bizarre behavior	10.0 ± 5.2	10.9 ± 4.9	9.9 ± 6.2
(d) Thought disorder	11.2 ± 10.5	10.7 ± 9.8	9.6 ± 10.0
SANS global	20.5 ± 3.6	20.1 ± 4.3	18.9 ± 4.2
(a) Affective flattening	28.4 ± 6.8	27.9 ± 7.8	26.8 ± 7.1
(b) Alogia	10.2 ± 5.8	9.9 ± 5.6	9.7 ± 4.9
(c) Avolition	11.9 ± 3.6	12.0 ± 3.5	11.2 ± 3.5
(d) Anhedonia	16.0 ± 3.4	16.2 ± 3.2	15.1 ± 4.1
(e) Attention	5.1 ± 2.2	5.2 ± 2.4	5.2 ± 2.0

Table 1: Demographic and clinical data.

2.2 EEG recording

EEG was recorded from 64 electrodes using a Biosemi ActiveTwo amplifier (BioSemi, Netherlands) at a sampling rate of 1024 Hz. TMS was applied with a Magstim Rapid (Magstim, UK) and a figure-of-eight coil at a fixed strength of 80 percent maximal stimulator output. There were three recording sessions. Each session was recorded at the same time of day with one week between the sessions. In each session, there were two stimulation sites (above frontal and central-parietal electrodes, FC2 and either FC2 or CP2). At each of these sites, a real stimulation measurement was always coupled to a sham stimulation (by placing the TMS coil perpendicularly to the stimulation site). Each such measurement (e.g., real or sham stimulation over

FC2) comprised of around 100 single TMS pulses delivered manually at ∼3 s inter-pulse intervals. Each of the three stimulation sessions was preceded by a resting-state recording (duration mean±std: 260 s±60 s) in which subjects were requested to keep their eyes open. Here we report comparative analysis only for the real stimulation, as the sham stimulation is not relevant to the questions of this paper. Results are also only analyzed for stimulation over the FC2 electrode, as this stimulation site had the most complete data sets.

To maintain consistency between sessions, several measures were undertaken. First, the same EEG cap was used for all sessions with the exact same cap location. Second, a custom-built mobile, manually adjustable stand for the TMS coil was used in order to keep the coil position and orientation with respect to the FC2 electrode across sessions. Third, sessions were conducted at the same time of day and subjects were requested to maintain their sleep, coffee, and cigarette intake (which was monitored) constant for the days of the experiment. Furthermore, subjects listened to white noise through headphones during the sessions to reduce auditory distraction.

2.3 EEG data processing

Resting-state EEG and TMS-EEG data were processed offline in several steps. In the TMS-EEG datasets, two additional pre-processing steps were applied. First, the procedure of Freche et al. (2018) was used to remove the TMS-induced discharge artifacts, and subsequently, the data of 25 ms duration following the TMS-pulse application, which could not be easily reconstructed at this sampling rate, were linearly interpolated. Afterwards, all datasets were high-pass filtered at 1 Hz and low-pass filtered at 150 Hz followed by a notch filter at 50 Hz using FIR filters by applying EEGLabs eegfiltnew function. Bad electrodes were removed from any further analysis following visual inspection. Remaining artifacts due to muscle activity, eye blinks, etc. were removed using Independent Component Analysis (ICA). The TMS-EEG data were subsequently epoched into trials for a time window of 1 s before and 2 s after each pulse. Finally, EEG signals were re-referenced by subtracting the signal average. In resting-state EEG datasets, only the first 182 s duration was used for further analysis. After further time-frequency decomposition (see Section 2.4, the 1 s at the beginning and at the end were removed to accommodate for edge effects. In the case of spectral power density computations (see Section 2.4), the beginning and ending seconds were also discarded to ensure the same length, even though there were no edge effects. Six datasets (5 sessions of different controls, 1 session of one patient) had a duration below 182 s and were therefore excluded from the resting-state EEG data analysis.

Care was taken during the data acquisition to ensure that the resting-state EEG recordings did not have any bad electrodes. However, in the TMS-EEG recordings, bad electrodes did occur, and in these datasets bad electrodes had to be removed, on average 1.3 electrodes in the controls group and 6.3 electrodes in the patients group, per dataset. About 50 % of the electrodes deleted were the FC2 electrode (stimulation site) or its nearest-neighbor electrodes, which were randomly prone to occasionally touching the coil.

2.4 Data analysis

2.4.1 Time-frequency decomposition, phase locking value (PLV), relative power, power spectral density

Time-frequency decompositions were computed using Morlet wavelets in the range of 2 Hz to 45 Hz with 2 cycles at the lowest and 15 cycles at the highest frequency in logarithmically spaced steps (cf. Bertrand et al. (2000)).

The PLV was computed from the phase of the time-frequency for each frequency and time point (Tallon-Baudry et al., 1996). It ranges between 0 and 1, where larger values indicate stronger phase locking between trials. The PLV was used to compare phases after the TMS pulse across trials.

Relative power was derived for each frequency, dividing by mean baseline power for baseline-normalization, and then converted to decibels. The baseline power was obtained as the mean power in the pre-stimulus window of 300 ms to 700 ms, averaged over all trials. This window falls outside the $2\sigma_t$-wide zone of influence of the trial boundaries and of the stimulation artifact, where σ_t is the (frequency-dependent) standard deviation in time of the Morlet wavelet (cf. Bertrand et al. (2000)).

For statistical analyses of the TMS-EEG data, time-frequency data were further processed in two steps. First, by down-sampling in time to 128 Hz and in frequency by averaging over the frequency bands, i.e. the delta (1-4 Hz), theta (4-8 Hz), alpha (8-12 Hz), beta (12-30 Hz), and gamma bands (30-45 Hz). Second, by averaging over time-frequency windows of interest. Furthermore, to reduce inter-trial variation, power was averaged over all trials of a given single session per subject. To take the same number of trials for every subject, only the first 70 trials surviving artifact removal were considered.

The power spectral density (PSD) was obtained for each electrode in the resting-state EEG by first computing the Fourier spectrum in a moving window of 2 s duration and 1 s overlap, and then taking the median of these windows.

The alpha peak location for each subject was obtained in the resting-state EEG by manual inspection of the average of the power spectral densities of all electrodes. For all three sessions of 1 control subject and one session of 1 patient, an alpha peak could not be detected, and therefore these subjects were not accounted for the peak location analysis.

2.4.2 Quartile coefficient of dispersion (QC)

According to the common view of EEG, there are two types of components that constitute the measured activity (Sauseng et al., 2007). One originates from spontaneous, ongoing activity, and is also called background activity. The other originates from short-lived and locally correlated bursts of synchronized activity such as event-related potentials. The first can be regarded as background noise and the second as intervals of modulated oscillatory signals.

Here we use a simple marker that can indicate whether modulated oscillations are present in a white noise signal. A common measure for the spread of a distribution based on its percentiles is the quartile coefficient (QC). Defining Q_1 as the percentile below which 25 percent of the distribution resides and Q_3 the corresponding value for the 75-th percentile, QC is defined by $(Q_3 - Q_1)/(Q_3 + Q_1)$. It is well-known that narrow-band-filtering of pure white noise yields a Rayleigh-distributed instantaneous amplitude (McClaning, 2012). This distribution has the property that its QC is independent of the amplitude of the underlying white noise, implying that the amplitude average is proportional to its fluctuation average. Furthermore, it has a known analytic expression with $QC_{Rayleigh} \approx 0.3741$. Thus, a signal with a QC different from $QC_{Rayleigh}$ implies the presence of non-noise components such as oscillatory signals.

For example, a pure-noise narrow-band signal with an additional constant oscillation at the mid-band frequency would increase the mean of the amplitude and hence the QC would be smaller than $QC_{Rayleigh}$. Another example is a pure-noise narrow-band signal with additional intervals of oscillatory bursts. This will increase the variation of the signal amplitude, leading to an increase in QC relative to $QC_{Rayleigh}$.

For the resting-state EEG analysis of Section 3.4, the QCs were derived for every frequency from 1 to 45 Hz from the time-frequency decomposition. For each electrode, the QCs were computed in a moving window of 40 s duration and 20 s overlap, and then the median of the QCs of all windows was taken.

2.4.3 Data visualization

All boxplots were plotted such that the box edges correspond to the 20-th to 80-th percentile of the underlying data. The center dot indicates the mean.

For visualization purposes, major electrode groups were aggregated and averaged. This constituted the following electrode aggregates: frontal-1 (FP1, FPz, FP2), frontal-2 (AF7, AF3, AFz, AF4, AF8), frontal-3 (F7, F5, F3, F1, Fz, F2, F4, F6, F8), frontal-4 (FT7, FC5, FC3, FC1, FCz, FC2, FC4, FC6, FT8), central-1 (T7, C5, C3, C1, Cz, C2, C4, C6, T8), central-2 (TP7, CP5, CP3, CP1, CPz, CP2, CP4, CP6, TP8), parietal-1 (P9, P7, P5, P3, P1, Pz, P2, P4, P6, P8, P10), parietal-2 (PO7, PO3, POz, PO4, PO8), occipital (O1, Oz, O2, Iz).

2.5 Statistical analysis

Each statistical analysis was performed at each electrode separately rather than correcting for multiple comparisons. The purpose of these single-electrode analyses was to evaluate phase and amplitude markers for correlated neural activity locally, i.e. at the single-electrode level, in the context of the noise hypothesis

as stated in the introduction. Furthermore, it allows to observe that the topographical distribution of all of the significantly different electrodes does not occur randomly on the head but rather follows physiologically reasonable patterns such as hemispheric symmetry or proximity to the TMS stimulation site.

Statistical comparisons of relative power and PLV were done for selected time-frequency windows and performed as follows. For each subject and each electrode, the quantity for the data inside the time-frequency window were averaged to a single number. To test for group differences for a given electrode, we used the following two-level model. The first level describes the session-specific effects, and the second the subject-specific effects. For a quantity Y_{ij} of session i and subject j,

$$\begin{aligned} &\text{level 1 (session-specific):} && Y_{ij} = \beta_{0j} + R_{ij} \\ &\text{level 2 (subject-specific):} && \beta_{0j} = \gamma_{00} + \gamma_{10}\, GROUP_j + U_{0j} \end{aligned}$$

where the factor $GROUP$ has the levels $Control$ and $Patient$. The model has the fixed effects γ_{00}, γ_{10} and the random effects R_{ij}, U_{0i} with $R_{ij} \sim N(0, \sigma)$, $U_{0j} \sim N(0, \tau_{00})$, where $N(a, b)$ denotes a normal distribution with mean a and standard deviation b. The effects R_{ij} capture between-session (i.e. within-subject) variability. The effects U_{0j} encapsulate the between-subject variability and also incorporate the assumption of homogeneity of subject variance. Model fitting and significance testing was done with Matlab's fitlme function. Notably, we repeated the statistical tests for Figs. 2B, 3B using the Wilcoxon rank sum test, which disregards the session structure. The results are very similar concerning the location of electrodes exhibiting a statistically significant difference between groups.

The same testing procedure was also applied to the comparison of the alpha peak locations in Figs. 4B.

Statistical tests for spectral power and quartile coefficients of instantaneous amplitudes were done using the Wilcoxon test, because the amplitude distribution is strongly skewed and non-Gaussian. Consequently, we ignored the dependence of sessions of each subject and instead treated them as 'independent subjects'.

3 Results

3.1 Power modulation due to the TMS pulse

Fig. 1 depicts the overall effect of the TMS pulse on the EEG amplitude. We computed time-frequency decompositions for each electrode and present the derived amplitudes in decibels, once as averages for the electrode aggregates (Fig. 1A, see Methods), and again as topographic plots of averages over consecutive time windows (Fig. 1B).

Three main qualitative effects are immediately apparent across the different time scales, ranging from tens of milliseconds to seconds and affecting several frequency bands. First, there is a reduction of the excitatory response in patients, which can be observed in two time-frequency windows. One is an immediate response to the TMS-pulse until around 300 ms in the delta, theta, and alpha bands (yellow and pinkish colors in Fig. 1B). The other appears in more central electrodes in the beta and gamma bands from around 500 ms to around 1 s (with white-pinkish in controls and white-bluish in patients, Fig. 1B).

The second effect is a facilitation of excitability, observable in two time-frequency windows. One is in the theta and alpha band, starting at around 300 ms and lasting at least until 1 s. The second occurs in the delta band after 700 ms until around 1.5 s. In controls, this effect appears as the bluish topographic plots in Fig. 1B, which are absent in patients.

The third effect we observe suggests a transition from a reduction in excitability in controls to facilitation of excitability in patients. This effect is visible in the time-frequency plots (mostly in the central-posterior-occipital electrodes), in the theta and alpha bands starting around 300 ms and lasting till around 1 s. It is also visible in the topographic plots that appear bluish (i.e. attenuated) in controls but have reddish (i.e. facilitated) additions for patients.

To quantify these three main effects, we delineated the time-frequency windows in which these effects are most pronounced and performed a post-hoc analysis in these windows. This is presented in Fig. 2. Alterations in response excitability are especially apparent in time-frequency window 2, where the mean power response at frontal, central, posterior, and occipital electrodes (midline FC-C-CP) turns from negative (power attenuation) in controls to positive (power facilitation) in patients. An electrode-wise comparison

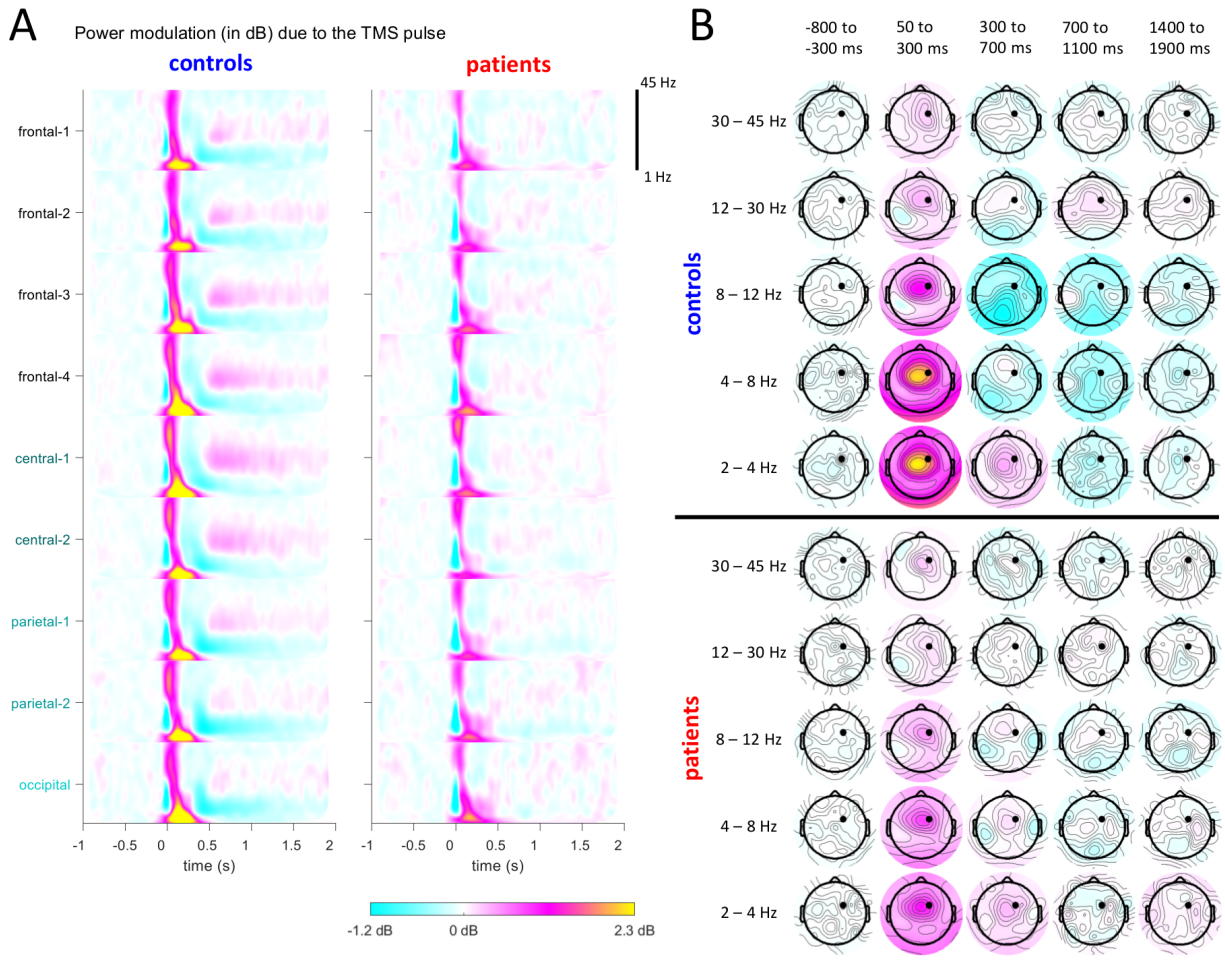

Figure 1: **A.** Time-frequency decompositions for electrode aggregates (averaged across trials). TMS was applied at time 0. The smearing in the time-frequency plot around time zero is due to the artifact removal process which introduces a gap of 25 ms in the data following the pulse onset. **B.** Topographical plots for different time-frequency windows (averaged over windows and across trials). The stimulation site FC2 is marked by a black dot.

between groups extracted the electrodes that showed statistical significant differences between patients and controls in each window.

The differential alterations of excitability that we verified with TMS-EEG in our patient group thus include a reduced excitability in early responses and a facilitated excitability as well as a shift from attenuation to facilitation of excitability in later responses.

3.2 Phase locking to the TMS pulse

We use the phase-locking value (PLV) to assess phase angle similarity following the TMS-pulse at each electrode separately, across trials. The phases were derived from the time-frequency decompositions used for Fig. 1. Fig. 3A shows the PLVs for each frequency and for all electrode aggregates, indicating that PLVs are generally reduced in patients. This is shown by a post-hoc analysis for the time-frequency windows of Fig. 3B. The PLVs, at all frequency bands, show most significant differences at more central and frontal electrodes, which are closest to the stimulation site, but also at posterior electrodes. We conclude that reduction of phase-locking to a stimulus can be verified with TMS-EEG in our patient group.

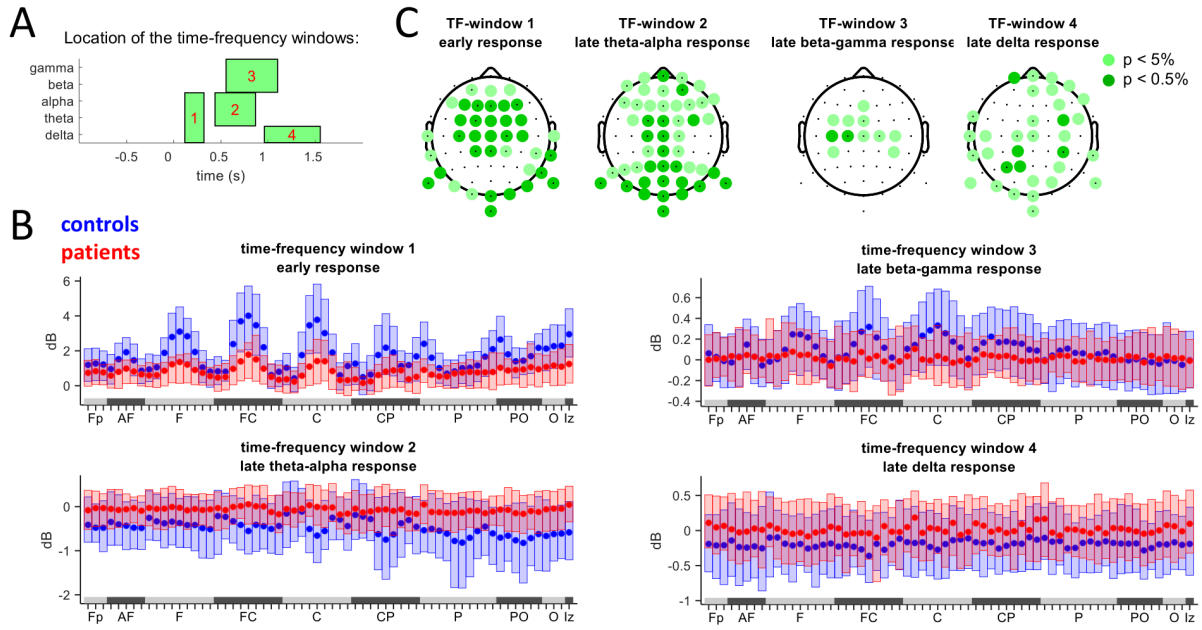

Figure 2: **A.** The different time-frequency windows that we consider for post-hoc statistical testing. **B.** Boxplots of the power values of each time-frequency window for each electrode (x-axis: 64 electrodes aggregated by groups. Order inside a group is band-wise from the right to left hemisphere.) **C.** Statistically significant group differences of power modulations. Each test was applied separately to each electrode.

3.3 Spectral power in resting-state EEG

The resting-state EEG was also assessed for differences in power spectra and amplitude fluctuations. The power spectral densities (PSDs) averaged for all electrode aggregates are depicted in Fig. 4A, with several alterations noticeable. There is an increase of power in lower frequency bands in patients and generally an elevated power in more frontal electrodes. Furthermore, the location of the mean alpha peak is shifted towards lower frequencies (controls 9.8±0.9 Hz, patients 9.0±0.8 Hz). Both effects are statistically significant (Figs. 4B-D), with the session effects ignored in this case (see Methods).

We conclude that the resting-state EEG spectrum of the patient group exhibits alterations from control spectra, especially in the frontal electrodes. Decomposition into frequency bands suggests that in most electrodes these effects are due to the theta band, while in frontal locations they occur also in the delta, beta, and lower gamma bands.

3.4 Amplitude fluctuations in resting-state EEG

We next tested for alterations in amplitude fluctuations at each frequency. A simple possible marker is the amplitude variation. It has to be normalized by the amplitude mean, which corresponds to the spectral power, because it shows large differences between subjects. This quantity is called coefficient of variation (CV). Because the CV is sensitive to outliers, in our analysis we replaced it by the similar but more robust quartile coefficient of dispersion (QC). Fig. 5A shows the QCs of the two subject groups averaged for different electrode aggregates. The QC of a pure white noise signal is denoted by $QC_{Rayleigh}$ and is shown as a dashed line. Deviations of the computed QCs from $QC_{Rayleigh}$ indicate the presence of signals that are non-noise (see Methods).

Boxplots for each electrode are shown in Fig. 5B, averaged over frequency bands. Two effects are evident. First, QCs of controls are generally larger in the alpha and beta range, whereas some differences exists in the delta and gamma bands, where patients show larger QCs. This is corroborated by statistical tests (Fig. 5C).

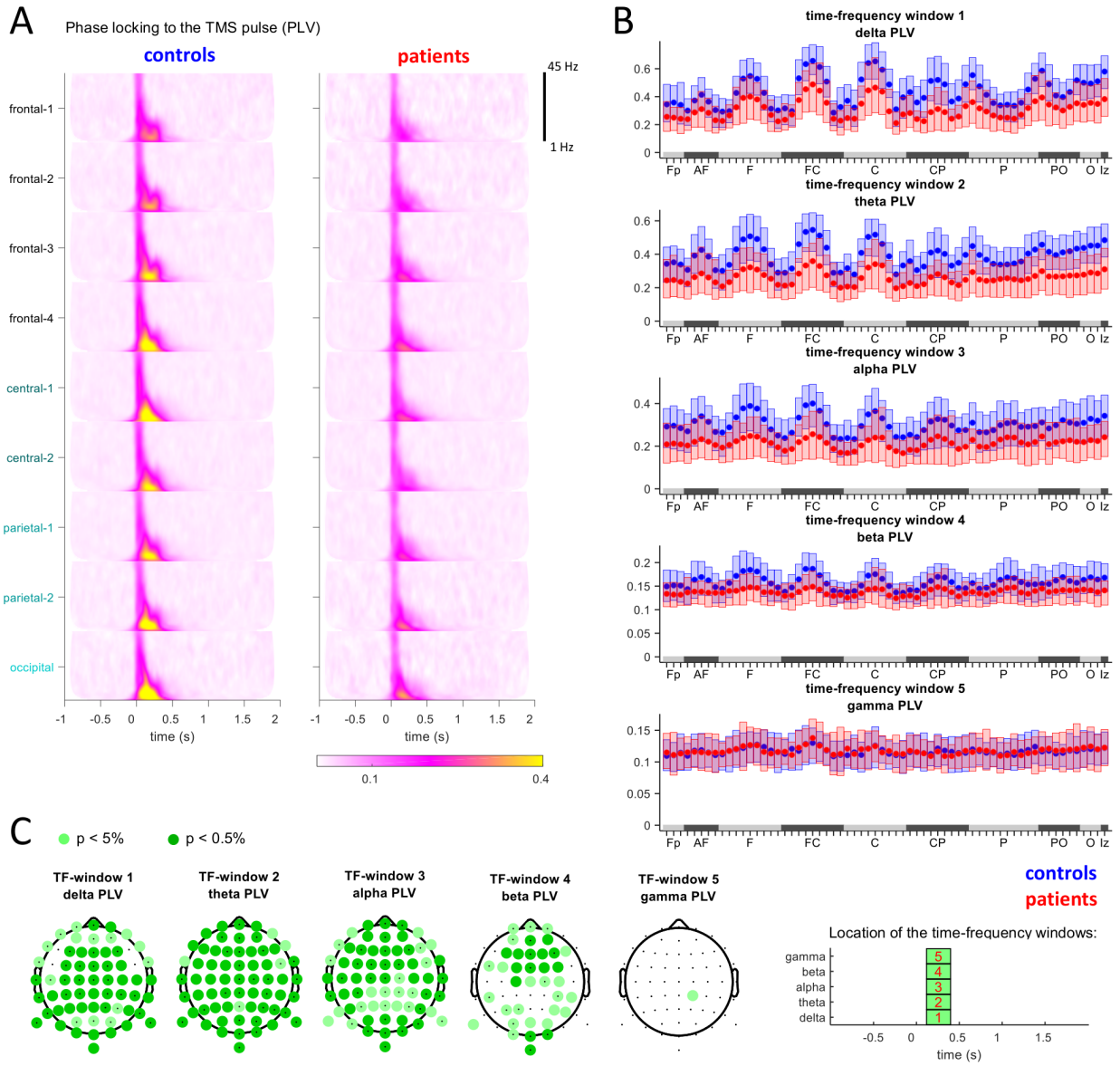

Figure 3: **A.** Phase locking value (PLV) for controls and for patients (displayed are averages of major electrode groups across trials). TMS was applied at time 0. **B.** Boxplots of the PLV values for selected time-frequency window, for each electrode. The time-frequency windows are specified in the bottom-right panel. **C.** Statistically significant group differences of PLV. Each test was applied separately to each electrode.

Second, the differences of the QCs between the groups do not coincide with differences of PSDs shown in Fig. 4.

We conclude that the resting-state EEG of the patient group exhibits a reduction of instantaneous amplitude fluctuations predominantly in the alpha and beta bands. In terms of the QC marker, the EEG in patients are closer to the value expected for random noise.

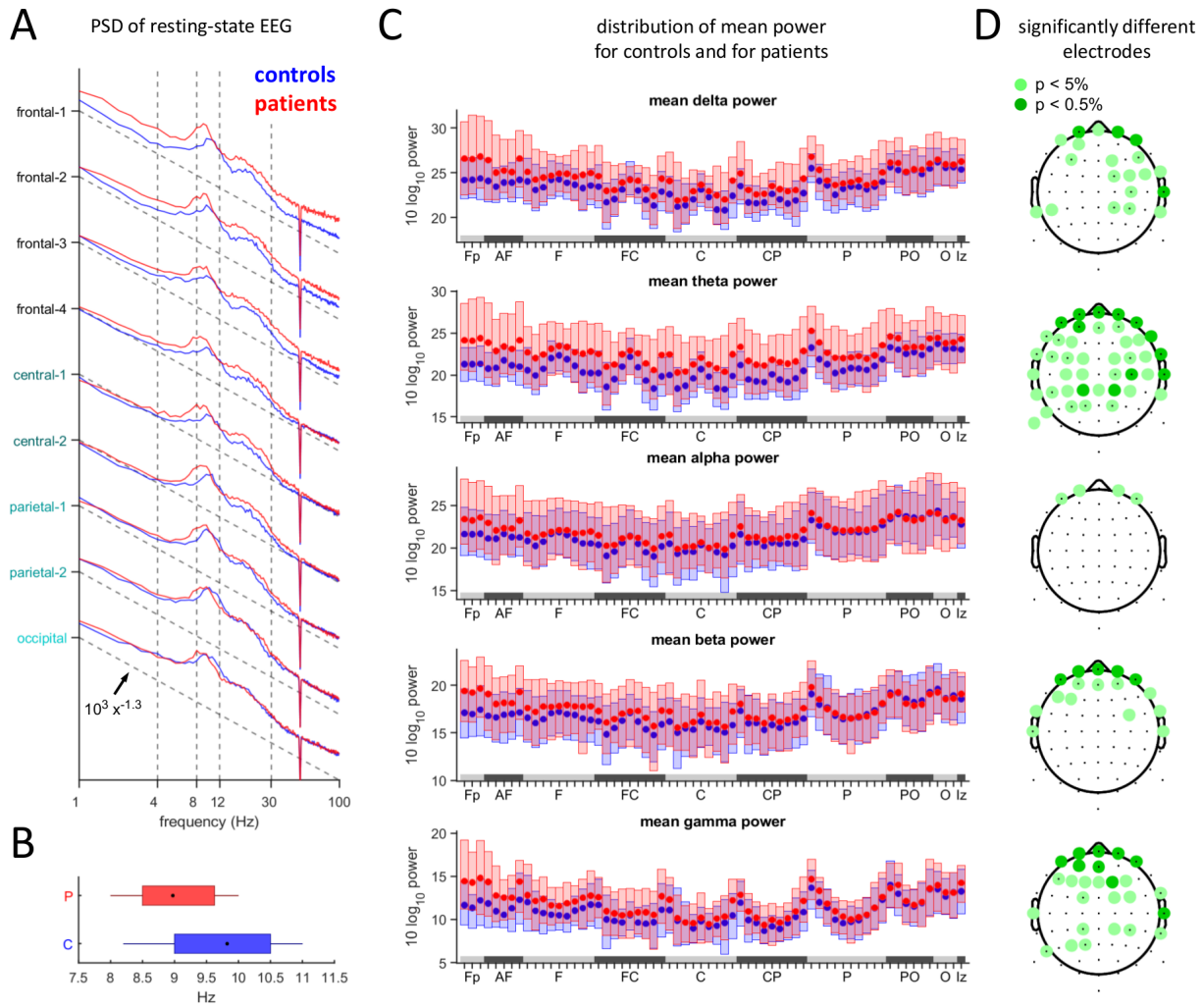

Figure 4: **A.** Log-log plots of resting-state EEG spectral power densities (PSDs) relative to a power law $10^3 x^{-1.3}$ (dotted line) for comparison. **B.** Alpha peak location for patients and controls. The black dot marks the mean, whiskers indicate the first and the third quartile. **C.** Boxplots of spectral power for the different frequency bands, for each electrode. **D.** Statistically significant group differences of spectral power in the different frequency bands. Test applied to each electrode separately.

4 Discussion

A hallmark of schizophrenia are profound, global alterations of brain activity (Uhlhaas and Singer, 2010). The previously suggested noise hypothesis (Winterer et al., 2000a; Rolls et al., 2008) on the underlying nature of these alterations postulates the existence of inherent noise in brain activity in schizophrenia that degrades the brains ability to form stable spatial and temporal correlations between cells and cell populations. Stated in this form, the hypothesis can be evaluated for stimulus-activated activity and for resting-state activity of the brain. We here investigated brain activity in schizophrenia by TMS-EEG and resting-state EEG. To strengthen the reproducibility of our results, we used three recording sessions for each subject, with one-week difference in between sessions. Our analysis of the TMS-evoked signals confirms previously reported findings of evoked response properties based on power modulations and phase locking. In addition, we find clear differences of the resting-state EEG, which appear in the spectral power and the instantaneous amplitude.

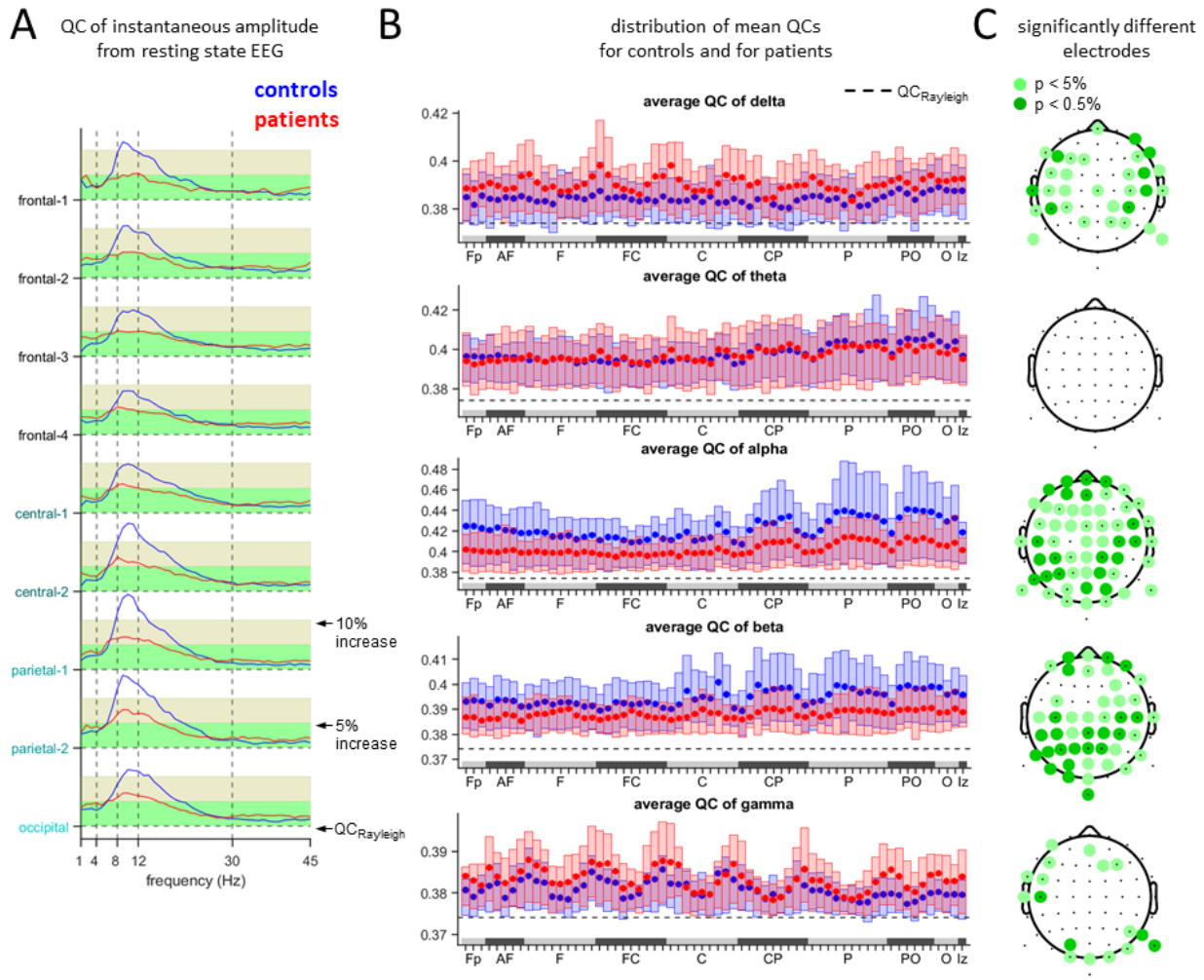

Figure 5: **A.** The quartile coefficient (QC) of the instantaneous amplitudes for different frequencies and electrode groups. The quartile coefficient $QC_{Rayleigh}$ of amplitude fluctuations of a Gaussian noise signal is marked by the horizontal dashed lines. **B.** Boxplots of the QCs for the different frequency bands, for each electrode. The quartile coefficient $QC_{Rayleigh}$ of white-noise amplitude fluctuations is marked by the horizontal dashed line. **C.** Statistically significant group differences of QCs in the different frequency bands. Test applied to each electrode separately.

Using a fluctuations analysis of the instantaneous amplitude, we demonstrate that the schizophrenia resting-state data looks more similar to pure random simulated noise than data from healthy controls. Overall, our results support the noise hypothesis in schizophrenia. In the context of the discussion to what extent is the intrinsic background activity in schizophrenia more oscillatory than random, we provide support for the notion of more randomness in the EEG of schizophrenia patients.

4.1 Alterations of evoked response processing

TMS application at frontal-central site FC2 evoked strong responses that lasted for well more than 1 s. Our focus on spatial and temporal correlations and their relation to the noise highlights that the power is modulated differently in the patient than in the control groups, in different time windows and frequency bands (Fig. 1). While in controls there was increased power in various frequency bands in early time-frequency

windows (Fig. 2A,B), in patients the power was reduced. This was different in later time-frequency windows, where patients exhibited increased power relative to the controls, which was strongest in the delta, theta, and alpha bands. The different time scales of the windows may be interpreted as different responses to the TMS, namely as direct, local activation of the pulse, and as late-stage, long-range responses activated by the direct response (Frantseva et al., 2012; Radhu et al., 2015; Rogasch et al., 2014). In this picture, the reduced signal-to-noise ratio may be interpreted as reduced excitability, and the facilitated excitability at later stages as reduction of inhibition. Together, this may be summarized as an altered excitation-inhibition balance.

These phenomena, observed in the response to the TMS, are consistent with the many known structural changes of brain tissue in schizophrenia. Indeed, alterations in connectivity have been reported (Krystal et al., 2017; Mikanmaa et al., 2019) during different developmental stages of the disease spectrum. Consistent with the excitability is a modification of local connectivity, such as a reduction of GABAergic cell density, myelination, connectivity, and alterations of gray matter density in progressed stages (Glahn et al., 2008). Consistent with alterations of signal propagation are abnormalities in long-range connectivity, such as changes of white-matter tracts (Tonnesen et al., 2018). In the context of TMS application, white matter integrity was demonstrated to directly influence how TMS-evoked activity spreads in the brain (Kearney-Ramos et al., 2018).

We then considered whether the power reduction of the responses are accompanied by a reduction in locking of phase to the pulse, based on an analysis of the PLV. Because both amplitude and PLV are related measures, this analysis is not independent of our findings regarding the changes in power. As expected, and reported previously for behavioral response paradigms (Winterer et al., 2000a, 2004; Spencer et al., 2003), schizophrenia patients exhibit a strong reduction of phase locking. Here we corroborate these findings using TMS, which has the advantage of being independent of subject cooperation and attention level (Daskalakis et al., 2002). Indeed, we observe a significant reduction of PLV in the delta, theta, alpha, and beta bands (Fig. 3). We note that the PLV can be artificially increased by volume conduction, which however would affect both groups to the same extent, and therefore these effects would work to reduce group differences rather than increase.

Our findings replicate previous reports for TMS-EEG in schizophrenia, such as Frantseva et al. (2012); Ferrarelli et al. (2012); Radhu et al. (2015); Ferrarelli et al. (2019); Rogasch et al. (2014); Shin et al. (2015) (see also Kaskie and Ferrarelli (2018) for a review), and confirm previous observations in behavioral evoked-response paradigms (Winterer et al., 2000a; Spencer et al., 2003). Alterations of long-range connections and inter-area synchronization in schizophrenia were reported in Hirvonen et al. (2017).

4.2 Alterations of resting-state power spectra

Various differences in the resting-state EEG spectra of schizophrenia patients were reported (Winterer et al., 2000a; Uhlhaas and Singer, 2010; Goldstein et al., 2015) though inconsistencies in the literature have been pointed out (Hunt et al., 2017; Newson and Thiagarajan, 2019). In our dataset, we identified a significant shift of the alpha peak to lower frequencies (slowing). This finding replicates previous reports (Goldstein et al., 2015; Garakh et al., 2012; Yeum and Kang, 2018; Murphy and Öngür, 2019), and may be related to symptoms (Garakh et al., 2012) or duration of illness (Goldstein et al., 2015). Other spectral power differences only appeared in frontal electrodes bands (Fig. 4A, B) with the exception of the theta band, which also shows differences in some parietal electrodes. However, the significant difference in theta power may be an artefact of our fixed definition of frequency bands together with the alpha peak slowing.

4.3 Neuronal noise and alterations of resting-state amplitude fluctuations

Beyond the differences in the spectra, several other alterations of the resting-state EEG in schizophrenia have been reported. This includes analyses of microstates (Rieger et al., 2016; Michel and Koenig, 2018), long range temporal correlations (LRTC) (Nikulin et al., 2012; Sun et al., 2014) and amplitude excursions (Sun et al., 2014). While the origin of these differences is not known, they are consistent with the noise hypothesis. We quantified the variability of resting-state amplitude fluctuations at different frequency bands in a simple and straightforward way, using the QC for moving time windows of 40 s. Significant differences

appear in several frequency bands (Fig. 5), most notably in the alpha and beta bands, which were previously reported to exhibit significant reductions of LRTC in schizophrenia (Nikulin et al., 2012).

QC is a measure similar to the coefficient of variation (CV), and can be viewed as evaluating the occurrence and strength of random events, that occur when the instantaneous amplitude deviates from the amplitude average. These deviations are therefore indicative of a short-lived, oscillatory event. A larger QC can be considered as representing a richer repertoire of events and hence of cortical activity, although it formally equals a noise-to-signal ratio. Support for this view comes from experimental measurements of the spiking activity in rodents (de Vasconcelos et al., 2017; Fontenele et al., 2019), in which the CV, computed on the timescale of tens of seconds, was used to characterize different cortical states.

A second interpretation of the QC that goes beyond the mere detection of group differences is that a signal with a QC that is closer to $QC_{Rayleigh}$ (see Methods) is indicative of increased randomness. However, this interpretation is not as straightforward and relies on additional assumptions.

The first assumption regards our model of the narrow-band filtered EEG signals, which we assume to be the sum of two parts. One part comprises the modulated oscillatory events and consists of oscillations around the center frequency of the band. The amplitude envelope of this part can vary slowly compared to the center frequency. The other part comprises of white noise with a constant strength. Hence, as the amplitudes of the event occurrences tend to zero, the QC of the instantaneous amplitude approaches that of a Rayleigh distribution.

The second assumption regards the relationship between amplitude and duration of the oscillatory event occurrences. Generally, the shorter the coverage by oscillatory events and the larger the event amplitudes, the larger is the QC. Furthermore, longer coverage by oscillatory events can make the QC very small, and even smaller than $QC_{Rayleigh}$ if the event amplitudes are large enough (see the examples discussed in Methods). So the interpretation that resting-state EEG activity is closer to noise is only true of we exclude the possibility that the majority of patients had rather long and rather strong occurrences of oscillatory events that are fine-tuned such that their QCs are close to $QC_{Rayleigh}$. In other words, this interpretation relies on the reasonable assumption that such very specific fine-tuning is unlikely.

4.4 Specificity of the investigated features for schizophrenia

In line with the literature, we report here statistically significant group-level differences between schizophrenia and healthy populations regarding evoked potentials in TMS-EEG, and regarding resting-state EEG. However, a subject-wise inspection of these properties shows that there is a large range of alterations and, importantly, a large overlap between the healthy range and the patient range (see e.g. the boxplots in Figs. 2-5). It is conceivable that specific values of various properties may be combined and achieve separable clustering in higher dimensions (Winterer et al., 2000b). This would give rise to a clear biomarker. However, based on the properties we investigated here, we could not achieve such a clear separation.

In fact, classification studies of intrinsic activity as well as evoked potentials in schizophrenia and psychosis indicate that achieving a comprehensive explanation linking alterations of intrinsic activity and evoked potentials would be difficult and complicated (Hudgens-Haney et al., 2017; Rolls et al., 2017). In fact, Clementz et al. (2017) suggested that there are three main different groups termed biotypes. These groups, which do not coincide with clinical classification schemes, were constituted from a battery of biomarkers. Hudgens-Haney et al. (2017) found different alterations, corresponding to the biotypes, in EEG background activity and in evoked potentials in an SSVEP-pro/antisaccade task paradigm. However, the origin of these phenomena is not clear. Still, it is consistent with our findings that there is a wide range of values for the properties that we considered here, overlapping with the range for healthy controls.

4.5 Limitations

The fact that the schizophrenia patients and the controls were not completely age-matched must be considered as a limitation. In particular, the younger ages in the control group are not optimal for strong conclusions. In addition, the patients in this study displayed differences in the direction their symptoms changed across sessions. Some displayed increase in symptoms, others decreased, while still others exhibited stationary symptoms across sessions. To see trends in the growth curves of the properties we measured,

variations of the study design may be required. One possibility is to increase the number of sessions beyond three. Another is to increase the inter-session time to more than one week, because all patients had experienced a recent episode and may have shown symptoms alterations over longer time durations.

Another limitation of the study was the imperfect repetition of coil placement across sessions. The coil position was determined using manual measurements and a customized stand, rather than with neuronavigation methods. This probably results in small deviations of coil placement between sessions. However, we expect these deviations to be distributed similarly in the two groups and not to be biased towards one group. Moreover, despite these expected deviations our results are robust across sessions, thus reducing the possibility that our findings are merely the result of a bias in coil placement. A third limitation of our study concerns the resting-state measurements that were both short (∼3-5 min) in duration and were only performed for open but not for closed eyes as well.

4.6 Conclusion

Our results corroborate and expand the previously reported evidence for the noise hypothesis in schizophrenia, obtained by investigating evoked potentials and resting state data. In TMS-EEG, we describe and confirm various alterations of evoked potentials. In resting-state EEG, we confirm alterations of amplitude fluctuations schizophrenia, using a new analysis based on a simple ratio measure of dispersion and mean. We suggest to distinguish between the extent of abnormal randomness and of abnormal oscillations in the brain activity, and note that this generalizes to both evoked potentials and resting-state EEG. A reasonable interpretation of our findings supports the possibility that the schizophrenia brain is characterized more by abnormal randomness.

5 Acknowledgements

NLB is supported by the Israel Science Foundation under Grant No. 1169/11, by the National Institute of Psychobiology in Israel, and by the Sagol Foundation (Israel). EM is supported by the Israel Science Foundation under Grant No. 1385/16, by the Minerva Foundation (Germany), and by the Clore Center for Biological Physics (Israel).

References

Diagnostic and Statistical Manual of Mental Disorders (DSM-IV-TR). American Psychiatric Association, Washington DC, 4 (text revision) edition, 2000.

N. C. Andreasen. *Scale for the assessment of negative symptoms (SAPS)*. University of Iowa, Iowa City, 1984.

N. C. Andreasen. The scale for the assessment of negative symptoms (SANS). *British Journal of Psychiatry*, 155:53 – 58, 1989. doi: 10.1192/S0007125000291502.

O. Bertrand, C. Tallon-Baudry, and J. Pernier. Time-frequency analysis of oscillatory gamma-band activity: Wavelet approach and phase-locking estimation. In C. Aine, G. Stroink, C. Wood, Y. Okada, and S. S.J., editors, *Biomag 96*, pages 919–922. Springer, New York, 2000. doi: 10.1007/978-1-4612-1260-7_224.

R. G. Bota, S. Munro, C. Nguyen, and A. Preda. *Course of Schizophrenia: What Has Been Learned from Longitudinal Studies?*, pages 281–300. Springer Netherlands, Dordrecht, 2011. doi: 10.1007/978-94-007-0831-0_11. URL `https://doi.org/10.1007/978-94-007-0831-0_11`.

B. A. Clementz, J. A. Sweeney, J. P. Hamm, E. I. Ivleva, L. E. Ethridge, G. D. Pearlson, M. S. Keshavan, and C. A. Tamminga. Identification of distinct psychosis biotypes using brain-based biomarkers. *Am J Psychiatry*, 173(4):373 – 384, 2017. doi: 10.1111/psyp.12875. URL `https://www.ncbi.nlm.nih.gov/pubmed/28419491`.

Z. J. Daskalakis, B. K. Christensen, P. B. Fitzgerald, and R. Chen. Transcranial magnetic stimulation. *J Neuropsychiatry Clin Neurosci.*, 14(4):406–415, 2002. doi: 10.1176/jnp.14.4.406.

N. A. P. de Vasconcelos, C. Soares-Cunha, A. J. Rodrigues, S. Ribeiro, and N. Sousa. Coupled variability in primary sensory areas and the hippocampus during spontaneous activity. *Scientific Reports*, 7:46077, 2017. doi: 10.1038/srep46077. URL `https://doi.org/10.1038/srep46077`.

A. A. Faisal, L. P. J. Selen, and D. M. Wolpert. Noise in the nervous system. *Nature Reviews Neuroscience*, 9:292 – 303, 2008. doi: 10.1038/nrn2258. URL `https://www.nature.com/articles/nrn2258`.

F. Ferrarelli, S. Sarasso, Y. Guller, B. A. Riedner, M. J. Peterson, M. Bellesi, M. Massimini, B. R. Postle, and G. Tononi. Reduced Natural Oscillatory Frequency of Frontal Thalamocortical Circuits in Schizophrenia. *JAMA Psychiatry*, 69(8):766–774, 08 2012. doi: 10.1001/archgenpsychiatry.2012.147. URL `https://doi.org/10.1001/archgenpsychiatry.2012.147`.

F. Ferrarelli, R. E. Kaskie, B. Graziano, C. C. Reis, and A. G. Casali. Abnormalities in the evoked frontal oscillatory activity of first-episode psychosis: A tms/eeg study. *Schizophrenia Research*, 206:436 – 439, 2019. doi: 10.1016/j.schres.2018.11.008. URL `http://www.sciencedirect.com/science/article/pii/S0920996418306388`.

A. J. Fontenele, N. A. P. de Vasconcelos, T. Feliciano, L. A. A. Aguiar, C. Soares-Cunha, B. Coimbra, L. Dalla Porta, S. Ribeiro, A. J. Rodrigues, N. Sousa, P. V. Carelli, and M. Copelli. Criticality between cortical states. *Phys. Rev. Lett.*, 122:208101, May 2019. doi: 10.1103/PhysRevLett.122.208101. URL `https://link.aps.org/doi/10.1103/PhysRevLett.122.208101`.

M. Frantseva, J. Cui, F. Farzan, L. V. Chinta, J. L. Perez Velazquez, and Z. J. Daskalakis. Disrupted Cortical Conductivity in Schizophrenia: TMSEEG Study. *Cerebral Cortex*, 24(1):211–221, 10 2012. doi: 10.1093/cercor/bhs304. URL `https://doi.org/10.1093/cercor/bhs304`.

D. Freche, J. Naim-Feil, A. Peled, N. Levit-Binnun, and E. Moses. A quantitative physical model of the tms-induced discharge artifacts in eeg. *PLOS Computational Biology*, 14(7):1–35, 07 2018. doi: 10.1371/journal.pcbi.1006177. URL `https://doi.org/10.1371/journal.pcbi.1006177`.

Z. V. Garakh, V. Y. Novototsky-Vlasov, Y. S. Zaitseva, A. B. Rebreikina, and V. B. Strelets. Frequency of the alpha activity spectral peak and psychopathological symptoms in schizophrenia. *Neurosci Behav Physi*, 42:1068, 2012. doi: 10.1007/s11055-012-9680-1. URL `https://link.springer.com/article/10.1007/s11055-012-9680-1`.

D. C. Glahn, A. R. Laird, I. Ellison-Wright, S. M. Thelen, J. L. Robinson, E. Lancaster, Jack LBullmore, and P. T. Fox. Meta-analysis of gray matter anomalies in schizophrenia: application of anatomic likelihood estimation and network analysis. *Biological Psychiatry*, 64(9):774 – 781, 2008. doi: 10.1016/j.biopsych.2008.03.031.

M. R. Goldstein, M. J. Peterson, J. L. Sanguinetti, G. Tononi, and F. Ferrarelli. Topographic deficits in alpha-range resting eeg activity and steady state visual evoked responses in schizophrenia. *Schizophrenia Research*, 168(1):145 – 152, 2015. ISSN 0920-9964. doi: 10.1016/j.schres.2015.06.012. URL `http://www.sciencedirect.com/science/article/pii/S0920996415003278`.

T. D. Habtewold, L. H. Rodijk, E. J. Liemburg, G. Sidorenkov, R. Bruggeman, and B. Z. Alizadeh. Schizophrenia symptoms are inherently heterogeneous: a systematic review of cluster and group-based studies. *bioRxiv*, 2019. doi: 10.1101/599498. URL `https://www.biorxiv.org/content/early/2019/04/07/599498`.

J. Hirvonen, M. Wibral, J. M. Palva, W. Singer, P. Uhlhaas, and S. Palva. Whole-brain source-reconstructed meg-data reveal reduced long-range synchronization in chronic schizophrenia. *eNeuro*, 4(5), 2017. doi: 10.1523/ENEURO.0338-17.2017. URL `https://www.eneuro.org/content/4/5/ENEURO.0338-17.2017`.

M. E. Hudgens-Haney, L. E. Ethridge, J. B. Knight, J. E. McDowell, S. K. Keedy, G. D. Pearlson, C. A. Tamminga, M. S. Keshavan, J. A. Sweeney, and B. A. Clementz. Intrinsic neural activity differences among psychotic illnesses. *Psychophysiology*, 54(8):1223–1238, 2017. doi: 10.1111/psyp.12875. URL https://www.ncbi.nlm.nih.gov/pubmed/28419491.

M. J. Hunt, N. J. Kopell, R. D. Traub, and M. A. Whittington. Aberrant network activity in schizophrenia. *Trends in Neurosciences*, 40(6):371 – 382, 2017. ISSN 0166-2236. doi: https://doi.org/10.1016/j.tins.2017.04.003. URL http://www.sciencedirect.com/science/article/pii/S016622361730070X.

R. E. Kaskie and F. Ferrarelli. Investigating the neurobiology of schizophrenia and other major psychiatric disorders with transcranial magnetic stimulation. *Schizophrenia Research*, 192:30 – 38, 2018. ISSN 0920-9964. doi: 10.1016/j.schres.2017.04.045. URL http://www.sciencedirect.com/science/article/pii/S0920996417302542.

T. Kearney-Ramos, D. Lench, M. Hoffman, B. Correia, L. Dowdle, and C. Hanlon. Gray and white matter integrity influence tms signal propagation: a multimodal evaluation in cocaine-dependent individuals. *Scientific Reports*, 8(1):3253, 2018. doi: 10.1038/s41598-018-21634-0.

L. J. Kerwin, C. J. Keller, W. Wu, M. Narayan, and A. Etkin. Test-retest reliability of transcranial magnetic stimulation eeg evoked potentials. *Brain Stimulation*, 11(3):536 – 544, 2018. ISSN 1935-861X. doi: 10.1016/j.brs.2017.12.010. URL http://www.sciencedirect.com/science/article/pii/S1935861X17310264.

J. H. Krystal, A. Anticevic, G. J. Yang, G. Dragoi, N. R. Driesen, X.-J. Wang, and J. D. Murray. Impaired tuning of neural ensembles and the pathophysiology of schizophrenia: A translational and computational neuroscience perspective. *Biological Psychiatry*, 81(10):874 – 885, 2017. URL https://doi.org/10.1016/j.biopsych.2017.01.004.

K. McClaning. *Wireless Receiver Design for Digital Communications*. SciTech Publishing, 2012.

C. M. Michel and T. Koenig. Eeg microstates as a tool for studying the temporal dynamics of whole-brain neuronal networks: A review. *NeuroImage*, 180:577 – 593, 2018. ISSN 1053-8119. doi: 10.1016/j.neuroimage.2017.11.062. URL http://www.sciencedirect.com/science/article/pii/S105381191731008X. Brain Connectivity Dynamics.

E. Mikanmaa, T. G. 't Jong, L. Hua, M. Recasens, H. Thune, and P. J. Uhlhaas. Towards a neurodynamical understanding of the prodrome in schizophrenia. *NeuroImage*, 190:144 – 153, 2019. ISSN 1053-8119. doi: 10.1016/j.neuroimage.2017.11.026. URL http://www.sciencedirect.com/science/article/pii/S1053811917309400. Mapping diseased brains.

M. Murphy and D. Öngür. Decreased peak alpha frequency and impaired visual evoked potentials in first episode psychosis. *NeuroImage: Clinical*, 22:101693, 2019. ISSN 2213-1582. doi: 10.1016/j.nicl.2019.101693. URL http://www.sciencedirect.com/science/article/pii/S2213158219300439.

J. Naim-Feil, A. Peled, D. Freche, S. Hess, A. Grinshpoon, N. Levit-Binnun, and E. Moses. Variability of dynamic patterns of cortical excitability in schizophrenia: A test-retest TMS-EEG study. 2019. (under review).

J. J. Newson and T. C. Thiagarajan. Eeg frequency bands in psychiatric disorders: A review of resting state studies. *Frontiers in Human Neuroscience*, 12:521, 2019. doi: 10.3389/fnhum.2018.00521. URL https://www.frontiersin.org/article/10.3389/fnhum.2018.00521.

V. V. Nikulin, E. G. Jönsson, and T. Brismar. Attenuation of long-range temporal correlations in the amplitude dynamics of alpha and beta neuronal oscillations in patients with schizophrenia. *NeuroImage*, 61(1):162 – 169, 2012. doi: 10.1016/j.neuroimage.2012.03.008. URL https://doi.org/10.1016/j.neuroimage.2012.03.008.

G. Northoff and N. W. Duncan. How do abnormalities in the brains spontaneous activity translate into symptoms in schizophrenia? from an overview of resting state activity findings to a proposed spatiotemporal psychopathology. *Progress in Neurobiology*, 145-146:26 – 45, 2016. ISSN 0301-0082. doi: 10.1016/j.pneurobio.2016.08.003. URL http://www.sciencedirect.com/science/article/pii/S0301008215300320.

N. Radhu, L. Garcia Dominguez, F. Farzan, M. A. Richter, M. O. Semeralul, R. Chen, P. B. Fitzgerald, and Z. J. Daskalakis. Evidence for inhibitory deficits in the prefrontal cortex in schizophrenia. *Brain*, 138(2): 483 – 497, 2015. doi: 10.1093/brain/awu360. URL https://www.ncbi.nlm.nih.gov/pubmed/25524710.

K. Rieger, L. Diaz Hernandez, A. Baenninger, and T. Koenig. 15 years of microstate research in schizophrenia — where are we? a meta-analysis. *Front Psychiatry*, 7:22, 2016. doi: 10.3389/fpsyt.2016.00022. URL https://www.ncbi.nlm.nih.gov/pubmed/26955358.

N. C. Rogasch, Z. J. Daskalakis, and P. B. Fitzgerald. Cortical inhibition, excitation, and connectivity in schizophrenia: a review of insights from transcranial magnetic stimulation. *Schizophrenia Bulletin*, 40(3):685 – 696, 2014. doi: schbul/sbt078. URL https://www.ncbi.nlm.nih.gov/pmc/articles/PMC3984517/.

E. T. Rolls, M. Loh, G. Deco, and G. Winterer. Computational models of schizophrenia and dopamine modulation in the prefrontal cortex. *Nature Reviews Neuroscience*, 9:696 – 709, 2008. doi: 10.1038/nrn2462. URL https://www.nature.com/articles/nrn2462.

E. T. Rolls, W. Lu, L. Wan, H. Yan, C. Wang, F. Yang, Y. Tan, L. Li, H. Yu, P. F. Liddle, and et al. Individual differences in schizophrenia. *BJPsych Open*, 3(6):265 – 273, 2017. doi: 10.1192/bjpo.bp.117.005058.

S. Rossi, M. Hallett, P. M. Rossini, and A. Pascual-Leone. Screening questionnaire before tms: An update. *Clinical Neurophysiology*, 122(8):1686, 2011. ISSN 1388-2457. doi: 10.1016/j.clinph.2010.12.037. URL http://www.sciencedirect.com/science/article/pii/S1388245710008692.

P. Sauseng, W. Klimesch, W. Gruber, S. Hanslmayr, R. Freunberger, and M. Doppelmayr. Are event-related potential components generated by phase resetting of brain oscillations? a critical discussion. *Neuroscience*, 146(4):1435 – 1444, 2007. doi: https://doi.org/10.1016/j.neuroscience.2007.03.014. URL http://www.sciencedirect.com/science/article/pii/S0306452207003314.

K. S. Shin, J. S. Kim, S. N. Kim, K. S. Hong, B. F. O'Donnell, C. K. Chung, and J. S. Kwon. Intraindividual neurophysiological variability in ultra-high-risk for psychosis and schizophrenia patients: single-trial analysis. *Npj Schizophrenia*, 1:15031, 2015. doi: 10.1038/npjschz.2015.31. URL https://doi.org/10.1038/npjschz.2015.31.

K. M. Spencer, P. G. Nestor, M. A. Niznikiewicz, D. F. Salisbury, M. E. Shenton, and R. W. McCarley. Abnormal neural synchrony in schizophrenia. *Journal of Neuroscience*, 23(19):7407–7411, 2003. doi: 10.1523/JNEUROSCI.23-19-07407.2003. URL https://www.jneurosci.org/content/23/19/7407.

J. Sun, Y. Tang, K. O. Lim, J. Wang, S. Tong, H. Li, and B. He. Abnormal dynamics of eeg oscillations in schizophrenia patients on multiple time scales. *IEEE Transactions on Biomedical Engineering*, 61(6): 1756–1764, June 2014. ISSN 0018-9294. doi: 10.1109/TBME.2014.2306424.

C. Tallon-Baudry, O. Bertrand, C. Delpuech, and J. Pernier. Stimulus specificity of phase-locked and non-phase-locked 40 hz visual responses in human. *Journal of Neuroscience*, 16(13):4240 – 4249, 1996. doi: 10.1523/JNEUROSCI.16-13-04240.1996. URL https://www.jneurosci.org/content/16/13/4240.

S. Tonnesen, T. Kaufmann, N. T. Doan, D. Alns, A. Cordova-Palomera, D. v. d. Meer, J. Rokicki, T. Moberget, T. P. Gurholt, U. K. Haukvik, T. Ueland, T. V. Lagerberg, I. Agartz, O. A. Andreassen, and L. T. Westlye. White matter aberrations and age-related trajectories in patients with schizophrenia and bipolar disorder revealed by diffusion tensor imaging. *Scientific Reports*, 8(1):14129, 2018. doi: 10.1038/s41598-018-32355-9. URL https://www.nature.com/articles/s41598-018-32355-9.

P. J. Uhlhaas and W. Singer. Abnormal neural oscillations and synchrony in schizophrenia. *Nature Reviews Neuroscience*, 11(2):100 – 113, 2010. URL https://doi.org/10.1038/nrn2774.

G. Winterer, M. Ziller, H. Dorn, K. Frick, C. Mulert, Y. Wuebben, W. Herrmann, and R. Coppola. Schizophrenia: reduced signal-to-noise ratio and impaired phase-locking during information processing. *Clinical Neurophysiology*, 111(5):837 – 849, 2000a. doi: 10.1016/S1388-2457(99)00322-3. URL http://www.sciencedirect.com/science/article/pii/S1388245799003223.

G. Winterer, M. Ziller, H. Dorn, K. Frick, C. Mulert, Y. Wuebben, and W. M. D. Herrmann. Frontal dysfunction in schizophrenia — a new electrophysiological classifier for research and clinical applications. *European Archives of Psychiatry and Clinical Neuroscience*, 250:207–214, 2000b. doi: 10.1007/s004060070026.

G. Winterer, R. Coppola, T. E. Goldberg, M. F. Egan, D. W. Jones, C. E. Sanchez, , and D. R. Weinberger. Prefrontal broadband noise, working memory, and genetic risk for schizophrenia. *Am J Psychiatry*, 161 (3):490–500, 2004. doi: 10.1176/appi.ajp.161.3.490.

T.-S. Yeum and U. G. Kang. Reduction in alpha peak frequency and coherence on quantitative electroencephalography in patients with schizophrenia. *J Korean Med Sci*, 33(26):e179, 2018. doi: 10.3346/jkms.2018.33.e179. URL https://www.ncbi.nlm.nih.gov/pmc/articles/PMC6010743/.